

1 **Supplementary material**

2 **Global patterns and drivers of influenza decline during the**
3 **COVID-19 pandemic**

4 Francesco Bonacina^{1,2}, Pierre-Yves Boëlle¹, Vittoria Colizza^{1,3}, Olivier Lopez², Maud
5 Thomas², Chiara Poletto¹

6 ¹INSERM, Sorbonne Université, Pierre Louis Institute of Epidemiology and Public Health, Paris, France

7 ²Sorbonne Université, CNRS, Laboratoire de Probabilités, Statistique et Modélisation, LPSM, Paris, France

8 ³Tokyo Tech World Research Hub Initiative (WRHI), Tokyo Institute of Technology, Tokyo, Japan

9 Corresponding author: Chiara Poletto (chiara.poletto@inserm.fr)

10	Additional methods	2
11	Definition of trimesters	2
12	Details on the computation of the log relative influenza level	2
13	Definition of covariates	2
14	Algorithms for the regression analysis	7
15	Additional results	8
16	Countries included in the analysis	8
17	Regression tree	8
18	Robustness checks and sensitivity analyses	14
19	Robustness of the variable selection procedure	14
20	Robustness of the tree structure optimization	14
21	Robustness of the tree under small perturbations of the dataset	14
22	Sensitivity of the variable selection under changes on the assumption made	14
23	Bibliography	16

24 **Additional methods**

25 **Definition of trimesters**

26 The trimesters considered in the analyses are periods of 13 weeks, defined so that the
27 winter trimester best covers the typical period of flu epidemics in northern countries.
28 Northern countries are defined as countries with latitude above the Tropic of Cancer. The
29 winter trimester is identified based on FluNet data from 1995 to 2019, as follows. For each of
30 the 365 possible starting dates of the trimester (a window of 91 days), we computed the
31 annual proportion of positive cases falling in the period, averaged over all northern countries
32 and years. We then define the winter trimester as the one that contains the highest annual
33 proportion of positive cases. The spring, summer and autumn trimesters are identified
34 accordingly. Also, we verified that the summer trimester according to this definition roughly
35 contains the highest proportion of positive cases for southern countries. The winter, spring,
36 summer and autumn trimesters obtained begin the first Monday following 12 December, 12
37 March, 11 June and 11 September, respectively. Certain years have 53 weeks instead of 52,
38 thus trimesters may occasionally have 14 weeks.

39 **Details on the computation of the log relative influenza level**

40 Data reported on FluNet were partial or not consistent in some cases. Number of processed
41 tests was sometimes different from the sum of positive and negative tests. In this case, the
42 sum of positive and negative tests was used as the number of processed tests. When one of
43 the three records (processed, positive and negative tests) was missing, this could be
44 computed from the other two. The number of processed tests, when missing, was computed
45 from the sum of positive and negative tests, the number of positive tests, when missing, was
46 computed from the difference between processed and negative tests (provided the former
47 was larger or equal to the later), and so on. We discarded weeks in which only processed
48 and either positive or negative tests were present and the number of processed tests was
49 smaller than the number of positive/negative tests. We also discarded weeks with only one
50 record. Russia showed some irregularities with certain weeks having the number of
51 processed tests nearly equal to the number of positive tests differently from the preceding or
52 following weeks, signalling sudden changes in the data collection and sharing protocol.
53 These weeks were removed from the analysis.

54 Before calculating the percentage of positive influenza tests, 0.5 positive cases are added to
55 each country-trimester, so that the positivity rate always results greater than zero. This
56 allows distinguishing countries without influenza and with a massive surveillance system
57 from countries without influenza but processing only a few tests.

58 When working with percentages - e.g. the percentage of influenza positive samples or the
59 percentage of annual influenza samples falling in a certain trimester - the centre of the
60 distribution was computed from the closure of the geometric mean, that was proved to be a
61 BLU (best linear unbiased) estimator, unlike the standard arithmetic mean [1].

62 **Definition of covariates**

63 Definition of the covariates included in the main analyses:

- 64 • **age**: median age of population, UN projection for 2020.

- 65 • **longitude**: longitude of the centre of population of the country in degrees, from -180
66 (W) to 180 (E). Longitude of the country is computed as the average longitude of all
67 the cities of the country with more than 300K inhabitants. The average is weighted for
68 the population size of each city. If there are no cities in the country with at least 300K
69 inhabitants, the longitude of the capital is considered.
- 70 • **latitude**: latitude of the centre of population of the country in degrees, from -90 (S) to
71 90 (N). The latitude is calculated analogously to *longitude*.
- 72 • **T**: average temperature (in Celsius degrees) of the country-trimester. For each
73 country, the temperature is computed as the average temperature of all the cities
74 within the country with more than 300K inhabitants, weighted by the population size.
75 If there are no cities in the country with at least 300K inhabitants, the capital is
76 considered. Temperature data are taken from the ERA5 dataset, which provides
77 hourly estimates of weather variables for all locations identified by a regular lat-lon
78 grid of 0.25 degrees. The temperature of a city is calculated by looking at the closest
79 grid point to the city and averaging the temperatures for the hours 0h00, 6h00, 12h00
80 and 18h00 of each day of the trimester.
- 81 • **RH**: average relative humidity, computed analogously to the *temperature*.
- 82 • **IDVI**: Score for the preparedness of a country in facing infectious diseases, from 0
83 (most vulnerable) to 1 (less vulnerable).
- 84 • **COVID-19 daily cases**: number of reported daily cases of COVID-19 per million of
85 inhabitants averaged over the trimester.
- 86 • **workplace presence reduction**: median over the trimester of the daily percentage
87 reduction of presence at workplaces.
- 88 • **reduction of international flights**: average percentage of reduction in the inbound
89 and outbound air passengers of the country for each trimester with respect to the
90 same trimester of 2019. The reduction for a trimester is calculated as the weighted
91 average of the monthly reduction for the 4 months covering the trimester, with first
92 and last months of the trimester, partially covered by the trimester, weighted 0.5,
93 while the other months, fully covered by the trimester, weighted 1. The reduction for
94 the month m and year $y=2020,2021$ is defined as $1 - w_{m,y}/w_{m,2019}$, with w being the
95 number of passengers flying to or from the country.
- 96 • **nb days of school closure**: number of days over the trimester when policies related
97 to schools and universities closure were implemented. The OxGRT dataset provides
98 2 daily variables: (i) the level of severity of the policy as measured on an ordinal
99 scale (0=no measure, 1=altered openings for schools, 2=closing certain
100 levels/categories of schools, 3=complete closure), and (ii) the geographical scope,
101 i.e. whether that policy is enforced locally or nationally. Based on the values of these
102 variables different definitions of school closure are possible - severity equal or above
103 1, 2, or 3, and each of these severity levels being implemented either locally or
104 nationally. To choose the most convenient definition we used an unsupervised
105 approach. We first computed the number of days with school closure for each data
106 point (country-trimester) for all possible definitions. We then computed the
107 distribution of the number of days with school closure over all data points and picked
108 the definition with maximum resolution power, i.e. that maximises the number of
109 observations with values not falling in the extremes. We obtained that schools are
110 considered to be closed if certain levels/categories of schools were closed on a
111 national scale or if there was at least one complete closure on a local scale.
- 112 • **nb days of workplace closure**: The severity levels defined in the OxGRT dataset
113 were: 0=no measures, 1=recommend closings, 2=require closing for some
114 sectors/categories of workers, 3=require closing for all-but-essential workplaces.
115 With the unsupervised procedure described for school closure we obtained that

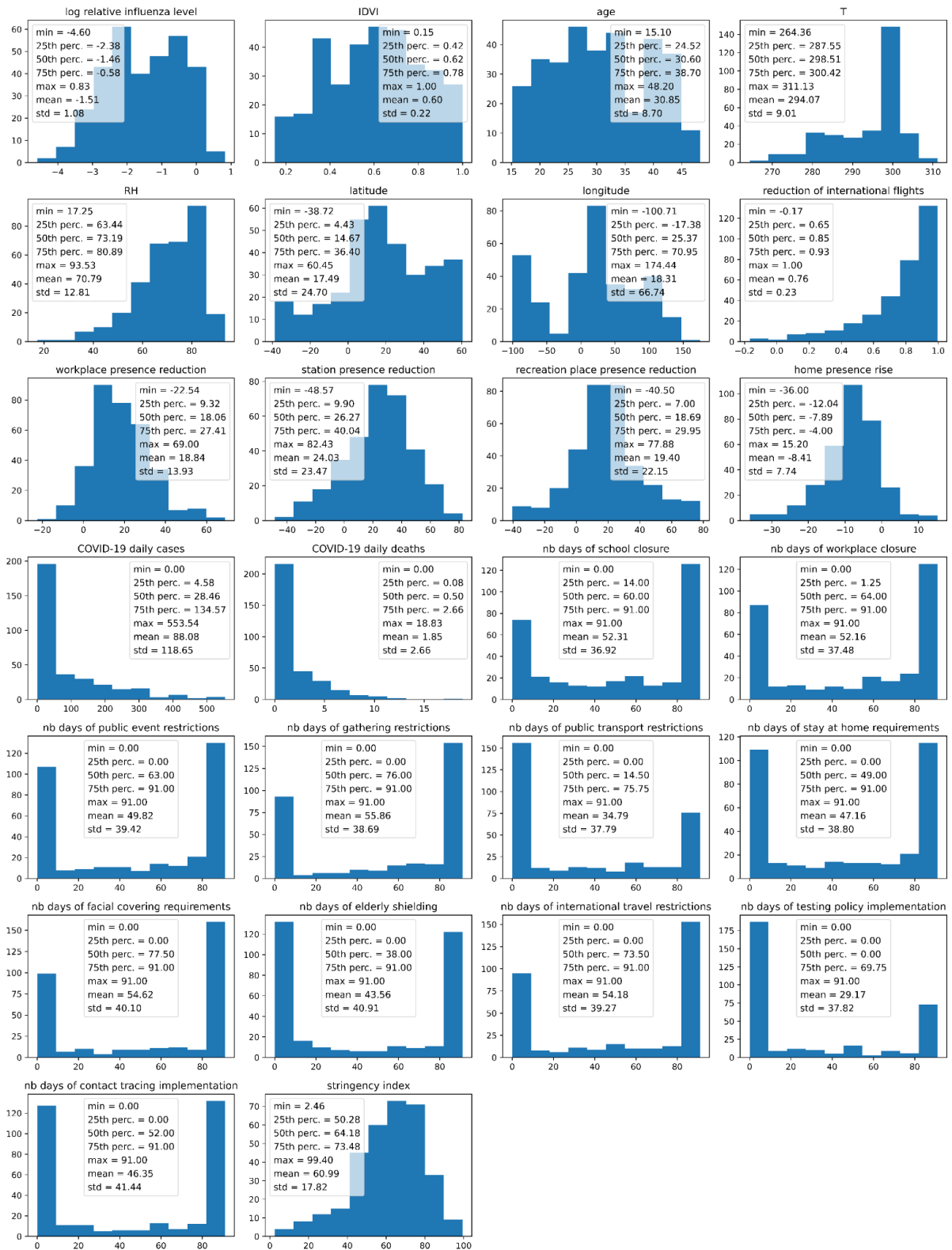
- 116 workplaces were defined as closed for stringency level at least 2 nationwide, or for
 117 stringency level 3 locally.
- 118 • **nb days of public event restrictions:** The severity levels defined in the OxGRT
 119 dataset were: 0=no measures, 1=recommend cancelling, 2=require cancelling. With
 120 the unsupervised procedure we obtained that public events were defined as closed
 121 when there was a countrywide enforcement.
 - 122 • **nb days of gathering restrictions:** The severity levels defined in the OxGRT
 123 dataset were: 0=no restrictions, 1=restrictions above 1000 people, 2=restrictions
 124 between 101-1000 people, 3=restrictions between 11-100 people, 4=restrictions on
 125 gatherings of 10 people or less. With the unsupervised procedure we defined as
 126 gatherings restriction a nationwide ban of gatherings of more than 100 people.
 - 127 • **nb days of public transport restrictions:** The severity levels defined in the OxGRT
 128 dataset were: 0=no measures, 1=recommend closing, 2=require closing. With the
 129 unsupervised procedure we obtained that public transports were defined as closed
 130 when a recommendation (level 1) was issued at local or national level.
 - 131 • **nb days of stay at home requirements:** The severity levels defined in the OxGRT
 132 dataset were: 0=no measures, 1=recommend not leaving house, 2= require not
 133 leaving house with exceptions for 'essential' trips, 3=require not leaving house with
 134 minimal exceptions. With the unsupervised procedure described for school closure
 135 we obtained that staying at home was implemented for severity level 1 or more,
 136 locally or nationally.
 - 137 • **nb days of international travel restrictions:** The severity levels defined in the
 138 OxGRT dataset were: 0=no restrictions, 1=screening arrivals, 2=quarantine arrivals
 139 from some or all regions, 3=ban arrivals from some regions, 4=ban on all regions or
 140 total border closure. With the unsupervised procedure we obtained that international
 141 travels were defined as enacted for severity level 3 or 4.
 - 142 • **nb days of facial covering requirements:** The severity levels defined in the
 143 OxGRT dataset were: 0=no policy, 1=recommended, 2=required in some specified
 144 shared/public spaces with other people present, 3=required in all shared/public
 145 spaces with other people present, 4=required at all times regardless of location or
 146 presence of other people. With the unsupervised procedure we obtained that mask
 147 use was implemented for severity level 3 or 4.
 - 148 • **nb days of testing implementation:** The severity levels defined in the OxGRT
 149 dataset were: 0=no testing policy, 1=only those who both (a) have symptoms AND
 150 (b) meet specific criteria, 2=testing of anyone showing COVID-19 symptoms, 3=open
 151 public testing. With the unsupervised procedure we obtained that testing policies
 152 were defined as implemented for stringency level 3.
 - 153 • **nb days of contact tracing implementation:** The severity levels defined in the
 154 OxGRT dataset were: 0=no contact tracing, 1=not for all cases, 2=contact tracing for
 155 all identified cases. With the unsupervised procedure we obtained that contact
 156 tracing was defined as implemented for severity level 2.
 - 157 • **nb days of elderly shielding:** The severity levels defined in the OxGRT dataset
 158 were: 0=no measures, 1=recommended isolation, hygiene, and visitor restriction
 159 measures in LTCFs and/or elderly people to stay at home, 2=narrow restrictions for
 160 isolation, hygiene in LTCFs, some limitations on external visitors and/or restrictions
 161 protecting elderly people at home, 3=extensive restrictions for isolation and hygiene
 162 in LTCFs, all non-essential external visitors prohibited, and/or all elderly people
 163 required to stay at home and not leave the home with minimal exceptions, and
 164 receive no external visitors. With the unsupervised procedure described for school
 165 closure we obtained that protection of elderly people was defined as implemented
 166 when it was enforced at least at level 2 locally or nationally.

167 Definition of the covariates included in the sensitivity analyses:

- 168 • **COVID-19 daily deaths:** number of reported daily deaths of COVID-19 per million of
 169 inhabitants averaged over the trimester.

- 170
- 171
- 172
- 173
- 174
- 175
- 176
- 177
- 178
- 179
- 180
- 181
- 182
- **station presence reduction:** median over the trimester of the daily percentage reduction of presence in public transport stations and transportation hubs.
 - **recreation place presence reduction:** median over the trimester of the daily percentage reduction of presence at restaurants, bars, shopping malls and other recreation places.
 - **home presence rise:** median over the trimester of the daily percentage rise of presence in residential places.
 - **stringency index:** average of the daily stringency index provided by OxCGRT. This index combines eight indicators of containment and closure policies and an indicator regarding the presence of public information campaigns related to the pandemic. The daily index ranges from 0 for countries with no measures, to 100 for countries adopting maximally stringent policies regarding all nine indicators. Seven of the eleven indicators considered in the previous covariates are included in this index.

183 Covariate distributions: We provide in Figure S1 the distributions of the log relative influenza
184 level and the covariates across countries-trimesters.



185 **Figure S1. Distributions of the 26 variables considered in the regression analysis, for all the 330**
 186 **observations included in the study.** For each plot, summary values of the distributions are shown in the
 187 legend. We included here both the covariates considered in the main analysis and the covariates considered in
 188 the sensitivity analysis.

189 Algorithms for the regression analysis

190 Clustering and regression trees: We relied on the CART algorithm [2] to classify countries-
191 trimesters based on a target variable, here the log relative influenza level. In a nutshell,
192 observations are iteratively split in groups according to a covariate selected at each iteration
193 so that the intra-group variance of the target variable is minimised. We controlled the
194 structure of the tree by fixing the minimum number of observations in a terminal leaf
195 (*minbucket*) and the regularisation parameter *cp* in the R package *rpart* [3]. The two
196 parameters are optimised by cross-validation.

197 Cross-Validation for the hyperparameter tuning of the regression tree: The search for the
198 optimal values of *minbucket* and *cp* is run over the following grid of parameters:
199 $minbucket \in \{4 \leq m \leq 18 \vee m \in N\}$ and $cp \in \{0.001 * c \vee 0 \leq c \leq 20, c \in N\}$. For each point of the
200 parameter space, 2000 trees were generated. Each tree is created on a random sample of
201 70% of the data and its prediction error (1-coefficient of determination) is calculated on the
202 remaining 30% of the observations. Following Breiman' rule, the optimal tree is identified as
203 the smallest tree that has mean prediction error less than the minimum error increased by its
204 standard deviation. The simplest tree is identified by looking at the smallest number of splits
205 on average, the largest *minbucket*, and the largest *cp*, in order. The optimal parameters
206 identified were *cp*=0.011, *minbucket*=4.

207 Variable selection through permutation risk measures for covariate importance: The Variable
208 Selection Using Random Forests (VSURF) algorithm has been exploited to identify the
209 predictors associated with the reduction of influenza. This method evaluates the importance
210 of each variable by measuring the prediction error increase when values of one variable at a
211 time are permuted. This is a classical method used in the framework of Random Forests
212 and, more in general, in machine learning algorithms. Also, some studies pointed out that
213 permutation risk measures of variable importance are often more effective than alternative
214 methods based on Sobol's indices or Shapley values [4].

215 The VSURF algorithm was run using the following parameters: *ntrees*=8000, *nfor.thres*=100,
216 *nfor.interpr*=100, *nfor.pred*=100 (and *mtry*=6 by default).

217 Additional results

218 Countries included in the analysis

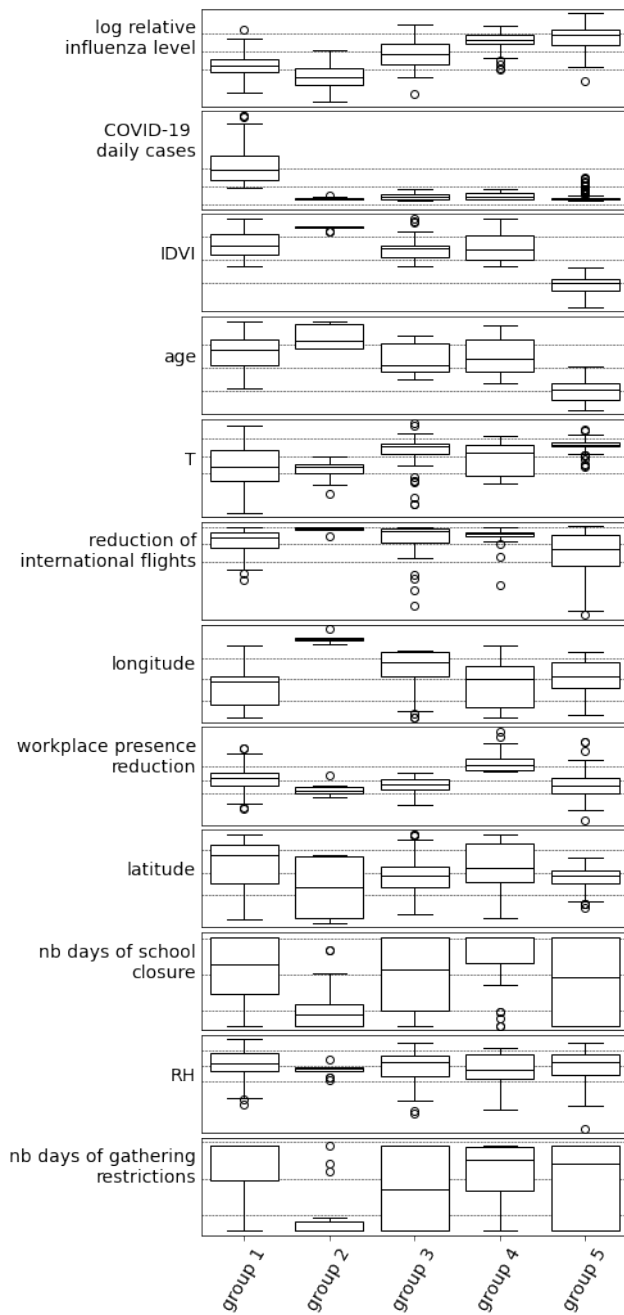
219 There were 166 countries that contributed to FluNet during the period from 15 Dec 2014 to
220 12 Sep 2021. All FluNet records for these 166 countries were included in Figure 1A. Upon
221 filtering based on the quality and extent of the FluNet records, 112 countries were included
222 in the descriptive study (Figure 1B and Figure 2). For those countries, only the trimesters
223 satisfying the inclusion criteria were included. Among the 112 countries, covariates were
224 available only for 93 countries. This last group of countries was included in the regression
225 analysis. The list of countries discarded at each step and included among the 93 countries
226 is reported in Table S1.

	countries in Fig. 1A (166)		countries in Fig. 1B and Fig. 2 (112)		countries for the regression analyses (93)	
Central and South America	AIA, ATG, ABW, BHS, BRB, BLZ, VGB, CYM, CUB, DMA, DOM, GUF, GRD, GLP, MTQ, KNA, LCA, VCT, SUR, TTO, TCA, VEN				ARG, BOL, BRA, CHL, COL, CRI, ECU, SLV, GTM, GUY, HTI, HND, JAM, MEX, NIC, PAN, PRY, PER, URY	
North America and Europe	BEL, BMU, CZE, GRC, MLT, MNE, NLD, SVK, CHE		ALB, ISL, OWID_KOS, MKD		AUT, BLR, BIH, BGR, CAN, HRV, DNK, EST, FIN, FRA, DEU, HUN, IRL, ITA, LVA, LTU, LUX, NOR, POL, PRT, MDA, ROU, RUS, SRB, SVN, ESP, SWE, UKR, GBR, USA	
Africa	BFA, CAF, TCD, MRT, MAR, RWA, SYC, SLE, SSD, TUN, ZWE		DZA, COD, ETH, GIN, MDG		AGO, CPV, CMR, COG, CIV, EGY, GMB, GHA, GNB, KEN, MLI, MUS, MOZ, NAM, NER, NGA, SEN, ZAF, SDN, TGO, UGA, TZA, ZMB	
Western, Central and South Asia	BHR, CYP, KWT, MMR, SYR, TJK, TKM, ARE, UZB, YEM		ARM, AZE, BTN, IRN, MDV, TLS, PSE		AFG, BGD, KHM, GEO, IND, IDN, IRQ, ISR, JOR, KAZ, KGZ, LAO, LBN, MYS, NPL, OMN, PAK, PHL, QAT, SAU, SGP, LKA, THA, TUR, VNM	
Eastern Asia and Oceania	FJI, PNG		CHN, PRK, NCL		AUS, JPN, MNG, NZL, KOR	

227 **Table S1. Countries included in the different steps of the study.** Countries are indicated with their 3-letter
228 code, OWID_KOS is for Kosovo. Countries are grouped into five regions, aggregating different influenza
229 transmission zones [5]: Central and South America (Temperate South America, Tropical South America and
230 Central America and Caribbean), North America and Europe (North America, Northern Europe, South West
231 Europe and Eastern Europe), Africa (Northern Africa, Western Africa, Middle Africa, Eastern Africa, Southern
232 Africa), Western, Southern and Central Asia (Western Asia, Southern Asia, South-East Asia, Central Asia),
233 Eastern Asia and Oceania (Eastern Asia, Oceania Melanesia Polynesia).

234 Regression tree

235 Additional details of the 5-group classification: We provide in the following additional details
236 on the 5-group repartition presented in Figure 4 of the main paper: the box plot of covariate
237 values for observations in each group (Figure S2), and the list of countries-trimester
238 belonging to each group (Table S2).

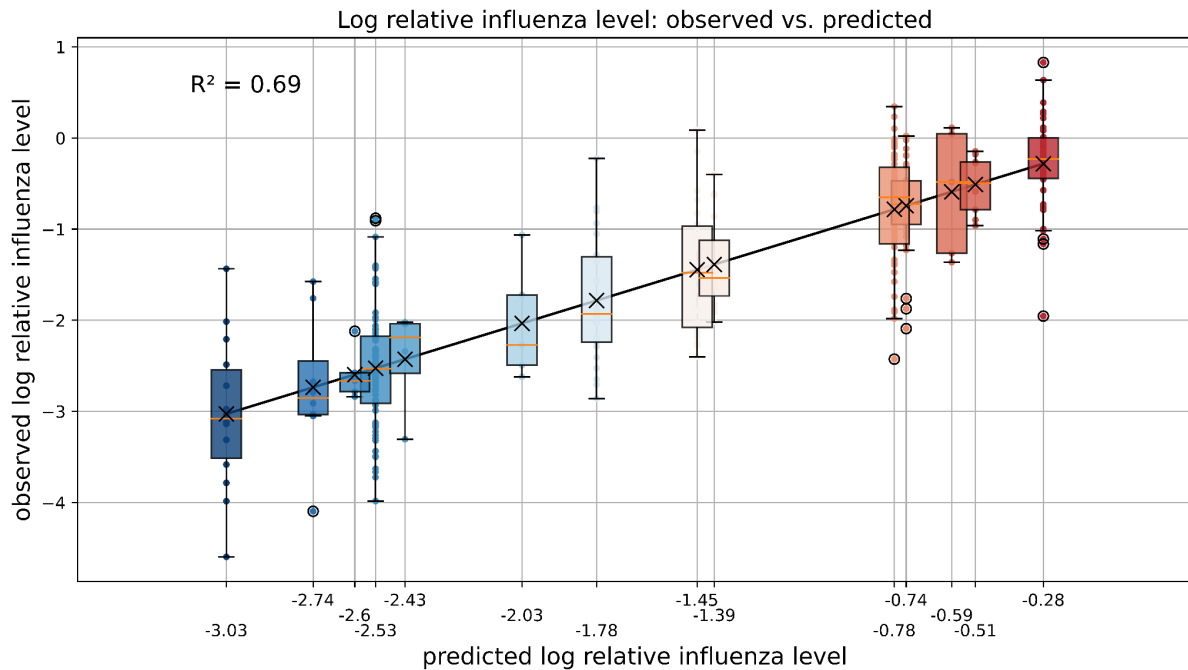


239 **Figure S2. Variable distributions for the five-group partitioning by means of the regression tree.** For each
 240 variable the boxplot shows the distribution in the group. Horizontal lines show median and quartiles of the whole
 241 dataset for comparison.

	Spring 2020	Summer 2020	Autumn 2020	Winter 2020-21	Spring 2021	Summer 2021
Group 1: leaves 1,2						
Central and South America	CHL	ARG, BRA, CHL, COL, CRI, PAN	ARG, CHL, COL, CRI	BRA, COL, CRI, MEX	ARG, BRA, CHL, COL, CRI, ECU, PAN, PER, PRY	ARG, BRA, CHL, COL, CRI, PAN, PRY, URY
North America and Europe			CAN, GBR, IRL, PRT, USA	AUT, BGR, BLR, CAN, DEU, DNK, ESP, EST, FRA, GBR, HRV, HUN, IRL, ITA, LUX, LVA, MDA, NOR, POL, PRT, ROU, RUS, SRB, SVN, SWE, UKR, USA	AUT, BLR, CAN, DEU, DNK, EST, HRV, IRL, LTU, LUX, LVA, MDA, NOR, POL, ROU, SVN, SWE, UKR, USA	
Africa		ZAF			GEO, JOR, LBN, MYS, OMN, QAT, TUR	ZAF
Western, Southern and Central Asia	QAT, SGP	QAT	ISR, JOR, LBN, OMN	GEO, ISR, JOR, LBN, QAT, TUR		LKA, MYS, PHL, THA
Eastern Asia and Oceania						
Group 2: leaf 3						
Central and South America						
North America and Europe						
Africa						
Western, Southern and Central Asia						
Eastern Asia and Oceania	AUS, JPN	AUS, NZL	AUS, JPN, KOR	AUS, JPN, KOR	AUS, JPN, KOR	AUS
Group 3: leaves 4,5,6,7						
Central and South America	BRA, PRY	PRY	MEX		MEX	ECU, PER, SLV
North America and Europe	SWE		NOR	FIN	RUS	
Africa		MUS	ZAF		ZAF	
Western, Southern and Central Asia	THA, VNM	IDN, LKA, MYS, THA, VNM	KAZ, MYS, QAT, SAU, SGP, THA, VNM	KAZ, LKA, SAU, SGP, THA, VNM	IDN, SAU, SGP, THA, VNM	QAT, SAU, SGP
Eastern Asia and Oceania	MNG			MNG		
Group 4: leaves 8,9						
Central and South America	ARG, COL, CRI, MEX, PAN, PER, SLV	SLV		ECU		
North America and Europe	AUT, CAN, DEU, DNK, EST, GBR, IRL, LVA, NOR, POL, ROU, RUS, SVN, UKR, USA				GBR	
Africa	MUS, ZAF					
Western, Southern and Central Asia	IDN, LKA, MYS, OMN, SAU	SGP	LKA	IDN, KGZ, OMN	LKA, PHL	
Eastern Asia and Oceania						
Group 5: leaves 10,11,12,13,14						
Central and South America	BOL, GTM, HND, HTI, JAM	HND, HTI, NIC	BOL, HND, HTI, NIC	GTM, HND, HTI	BOL, GTM, HND, HTI, JAM	GTM, HND, HTI, JAM, NIC
North America and Europe						
Africa	CIV, CMR, EGY, MLI, MOZ, TZA, ZMB	CIV, EGY, KEN, MLI, SEN, TZA, UGA, ZMB	CIV, CMR, EGY, GHA, KEN, NER, SEN, TGO, TZA, UGA, ZMB	CIV, CMR, EGY, GHA, KEN, NER, NGA, SEN, TGO, TZA, ZMB	CIV, CMR, EGY, GHA, KEN, MLI, NGA, SEN, TGO, TZA, UGA, ZMB	CIV, CMR, EGY, GHA, KEN, MLI, NGA, SEN, TGO, TZA, UGA, ZMB
Western, Southern and Central Asia	AFG, BGD, IND, KHM, LAO, NPL	BGD, KHM, LAO, NPL	AFG, BGD, IND, IRQ, KHM, LAO, NPL, PAK	AFG, IND, IRQ, KHM, LAO, NPL, PAK	AFG, BGD, IND, KHM, LAO, NPL, PAK	BGD, IND, KHM, LAO, NPL
Eastern Asia and Oceania						

242 **Table S2. Classification of countries-trimesters according to the high-level partitioning in five groups by**
243 **means of the regression tree.** Countries are grouped into five regions, aggregating different influenza
244 transmission zones [5]: Central and South America (Temperate South America, Tropical South America and
245 Central America and Caribbean), North America and Europe (North America, Northern Europe, South West
246 Europe and Eastern Europe), Africa (Northern Africa, Western Africa, Middle Africa, Eastern Africa, Southern
247 Africa), Western, Southern and Central Asia (Western Asia, Southern Asia, South-East Asia, Central Asia),
248 Eastern Asia and Oceania (Eastern Asia, Oceania Melanesia Polynesia).

249 **Full Regression Tree:** The regression tree selected using the algorithm had 14 terminal
250 leaves and a coefficient of determination $R^2=0.69$. The leaves identified by the model were
251 well defined (Figure S3), i.e. distinct from each other and characterised by homogeneous
252 values of log relative influenza level - only for two of them the interquartile width of the
253 observed log relative influenza level was greater than unity.



254 **Figure S3: Goodness of fit of the regression tree.** The 14 boxplots display the distributions of the log relative
 255 influenza level for countries-trimesters of the 14 leaves. The black crosses identify the mean values of the
 256 distributions (also shown through the color scale) that correspond to the predicted log relative influenza level. R^2
 257 is the coefficient of determination.

258 The tree is shown in Figure S4. The first four splits are done according to IDVI, COVID-19
 259 daily cases, longitude and workplace presence reduction as discussed in the main paper.
 260 The other variables are used for a finer partition in smaller groups. The classification of
 261 countries-trimesters in leaves is reported in the supplementary data [6].

262 Group 1 (109 observations) is split into leaves 1 and 2. In leaf 1, lower temperatures relative
 263 to leaf 2 are associated with a greater reduction in influenza. Leaf 1 consists largely of
 264 temperate countries in Europe, North and South America, during the 2020-2021 influenza
 265 season, which had a greater influenza reduction. Leaf 2 includes a more limited number of
 266 observations (26, compared with the 83 in leaf 1) from countries of tropical and subtropical
 267 areas with $IDVI > 0.54$, e.g. Panama, Costa Rica, Colombia, Malaysia. Influenza reduction for
 268 these countries was less strong compared with leaf 1, but still substantial if compared with
 269 low-IDVI tropical countries, classified in group 5.

270 Group 2 is formed by a single leaf with well defined properties detailed in the main paper.

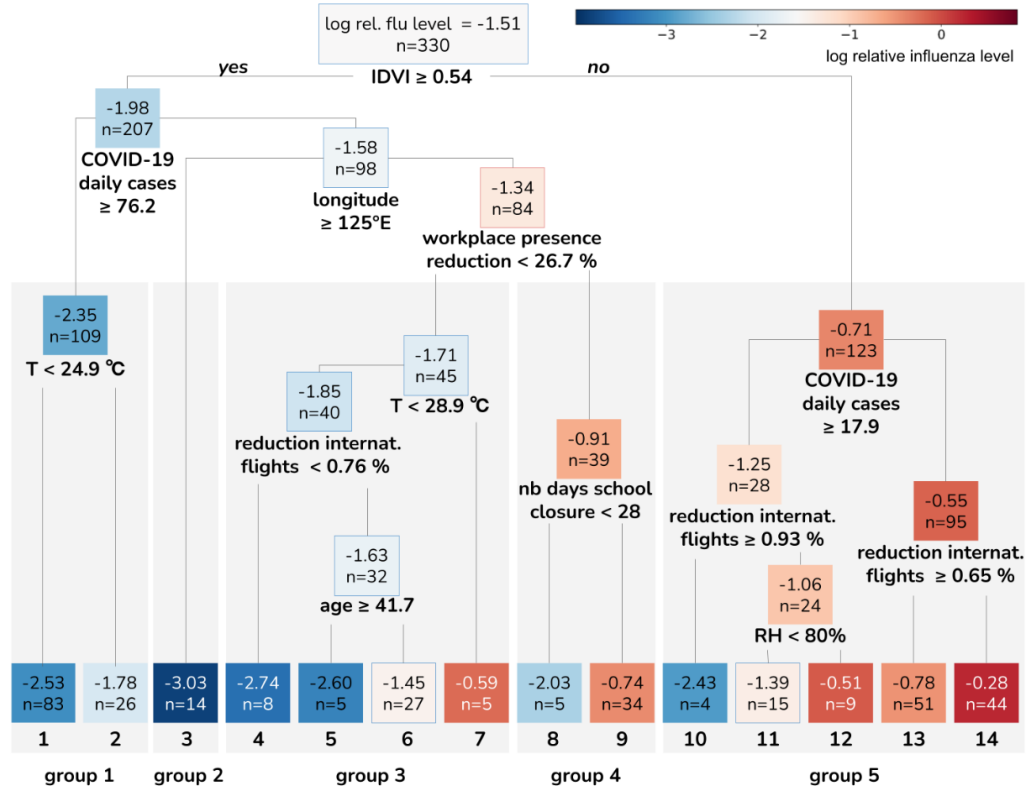
271 The 45 observations of the group 3 are distributed in four leaves including a few countries-
 272 trimesters each. Similarly to the split within group 1, a first split based on temperature
 273 separates countries with higher temperature and higher log relative influenza level (Saudi
 274 Arabia and Qatar) from countries with lower temperature and lower log relative influenza
 275 level. This second branch splits based on the reduction of international flights. On the left
 276 side of the split there is a group of 8 countries-trimesters where low values of log relative
 277 influenza level were associated with lower-than-average reduction of international flights,
 278 reduction of workplace presence and number of days with gathering restrictions. This group
 279 was characterised by a number of days of school closure higher than average. The right side

280 of the split has two leaves that are discussed in the main paper, i.e. leaf 5 including mainly
281 Singapore and leaf 6 including mainly other Southeast Asia countries.

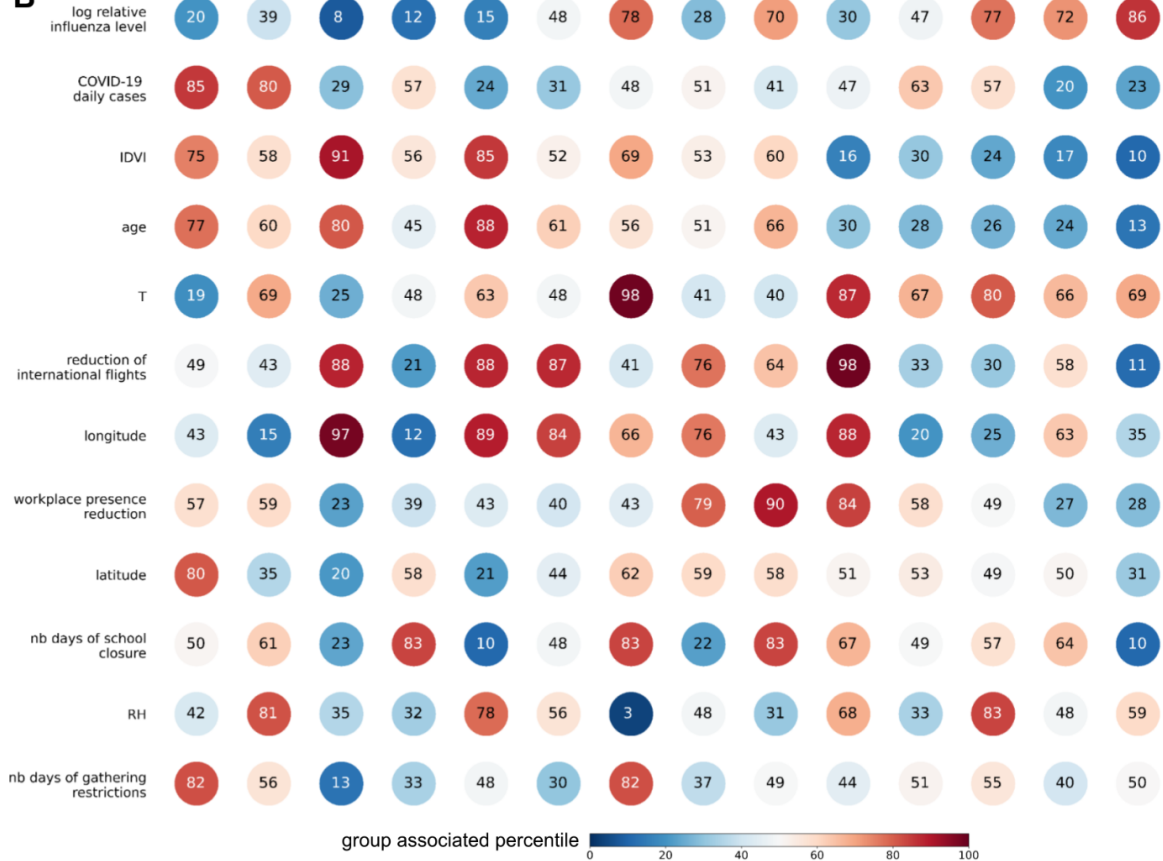
282 Group 4 consists of 39 observations. This includes mainly countries during spring 2020 that
283 are grouped in leaf 9 (34 out of 39 observations). Five observations are separated by the
284 other because they have a more limited number of days with school closure and a lower log
285 relative influenza level. This is a heterogeneous set of countries, mainly between winter
286 2021 and spring 2021.

287 Group 5 contains a significant proportion of all observations (123 out of 330) that are
288 separated into five leaves (leaves 10, 11, 12, 13 and 14). Interestingly, the five leaves show
289 a clear trend with increasing log relative influenza level that is, in general, associated with a
290 decrease in four of the five COVID-19 response variables - COVID-19 daily cases, reduction
291 of international flights, reduction of workplace presence, and number of days with school
292 closure. Limitations on gatherings remain moderate for all five leaves. Two splits are based
293 on the reduction of international flights, between leaf 10 and leaves 11 and 12, and between
294 leaf 13 and 14. For these two splits a greater reduction of international flights is associated
295 with a lower influenza log ratio. Finally, leaves 11 and 12 differ in relative humidity. The two
296 leaves contain almost the same set of countries for different trimesters - e.g. Guatemala,
297 Honduras, India, Nepal, and Zambia. These are tropical countries characterised by a dry and
298 a rainy season throughout the year, where influenza usually peaks twice a year with the
299 main peak during the rainy season [7–10]. Our analysis shows that for rainy seasons the
300 reduction of influenza was smaller.

A



B



301 **Figure S4: Full regression tree.** **A** Regression tree obtained with the variables selected in Figure 3. For each
 302 node the average log relative influenza level and the number of observations are reported (the former is also
 303 indicated with a colour scale). **B** Properties of each leaf. For each covariate the percentile of the whole dataset
 304 distribution the median of the group corresponds to is indicated with the colour scale and reported in the bubble.

305 **Robustness checks and sensitivity analyses**

306 **Robustness of the variable selection procedure**

307 The variable selection procedure is a stochastic algorithm that may lead to different results
308 when repeated. Therefore, variable importance was estimated by averaging over 100
309 stochastic realisations. To be sure results were stable we repeated the procedure 20 times.
310 Each time the same 11 predictors are selected as the important covariates for predicting the
311 log relative influenza ratios.

312 **Robustness of the tree structure optimization**

313 The regression tree was regularised by two parameters (*minbucket* and *cp*) optimised with
314 cross-validation through the stochastic procedure discussed in the Additional methods
315 section of the supplementary information. To be sure that the procedure converges to a
316 stable result we repeated it 10 times. The regularisation parameters selected each time were
317 very similar and led to the construction of trees almost identical to the tree described in the
318 Results section and in the supplementary information. In particular, the classification of
319 countries-trimesters in the five high-level groups was robust.

320 **Robustness of the tree under small perturbations of the dataset**

321 We assessed the robustness of the tree under small perturbations in the dataset. We built
322 ten regression trees on a random subsample of 314 observations (~95% of the total)
323 keeping the same 11 predictors and hyperparameters. The ten resulting trees (i.e. the
324 perturbed trees) were compared with the tree built from the entire dataset (i.e. the reference
325 tree) using the Adjusted Rand Index (ARI) [11]. Specifically, we compared the classification
326 in 5 groups to assess the robustness of the 5-group repartition discussed in the main paper.
327 The average score value for the ten comparisons is 0.86, indicating good agreement
328 between the perturbed and reference trees.

329 **Sensitivity of the variable selection under changes on the assumption made**

330 We tested whether the predictors of the log relative influenza level changed with the choices
331 made throughout the analysis. The creation of the dataset of observations is based on two
332 main assumptions: (i) $k=0.5$ positive cases had been added to each country-trimester in
333 order to remove zero counts of influenza cases, and (ii) a threshold $s=130$ for the minimum
334 number of tests processed per quarter was set to discard countries-trimesters with poor
335 data. In addition, some choices were made when defining the covariates. We tested the
336 robustness of our results to all these choices by analysing the following alternative models
337 (the baseline model is here referred as *base 0* model):

- 338 ● *base 1*: $k=1$ (instead of 0.5), $s=130$, same covariates of the base 0 model;
- 339 ● *base 2*: $k=0.5$, $s=26$ (instead of 130), same covariates of the base 0 model;
- 340 ● *base 3*: $k=0.5$, $s=260$ (instead of 130), same covariates of the base 0 model;
- 341 ● *Cov 1*: $k=0.5$, $s=130$, COVID-19 daily deaths is used in alternative to COVID-19 daily
342 cases to quantify the intensity of the COVID-19 epidemic;
- 343 ● *Mob 1*: $k=0.5$, $s=130$, the public transport station presence reduction is tested in
344 alternative to workplace presence reduction to capture changes of social activity;
- 345 ● *Mob 2*: $k=0.5$, $s=130$, the recreation place presence reduction is tested in alternative
346 to workplace presence reduction to capture changes of social activity;

- 347 ● *Mob 3*: $k=0.5$, $s=130$, the increase in home presence is tested in alternative to
348 workplace presence reduction to capture changes of social activity;
- 349 ● *No Age*: $k=0.5$, $s=130$, the variables age is removed among the set of covariates to
350 be included in the regression;
- 351 ● *No IDVI*: $k=0.5$, $s=130$, the variables IDVI is removed among the set of covariates to
352 be included in the regression;
- 353 ● *Str. Idx*: $k=0.5$, $s=130$, all variables associated with NPIs are replaced by the
354 stringency index.

355 For all the alternative models the selected sets of important factors are highly similar (Table
356 S3): impact of COVID-19, international mobility, workplace presence reduction (or the
357 alternative proxy of social activity considered), IDVI, age, temperature and longitude always
358 result significant, while latitude and RH are discarded only once and twice respectively. All
359 proxies of social activity tested were classified as important. The stringency index when
360 included was not selected, indicating that the aggregate information it carries is not important
361 in explaining the influenza reduction. This is consistent with the fact that only 2 out of the 11
362 governmental response variables were selected as important.

363 We used the ARI similarity index to compare the sensitivity trees and the baseline tree up to
364 the five-group repartitions. Models *Mob 1*, *Mob 2*, *Mob 3*, *No Age*, *Str. Idx.* led to an
365 excellent recovery of the baseline tree ($ARI > 0.9$). The 5-group repartition showed the same
366 behaviour as in the baseline model. The tree obtained with *Base 1* was in good agreement
367 with the baseline tree. Interestingly, removing IDVI from the set of covariates led to only a
368 moderate recovery of the baseline tree ($ARI= 0.69$), despite IDVI and Age being highly
369 correlated. Age is not able to fully compensate for IDVI in creating the 5 group repartition
370 discussed in the main paper. This is consistent with the fact that both covariates were found
371 to be important by the VSURF procedure.

372 The comparison of trees obtained with *base 2*, *base 3* and *Cov 1* and the baseline tree up to
373 the five-groups repartition led to lower similarity values (ARI between 0.53 and 0.66). Still,
374 we found that the four trees shared in large part the same behaviour. In particular, the first
375 split was the same (i.e. based on IDVI with the same threshold value), meaning that all
376 partitions had the distinction between high IDVI, low influenza countries and low IDVI, high
377 influenza ones. Also, the 2020 spring trimesters of temperate countries (comprising the bulk
378 of group 4) remained in great part grouped together and separated from the rest. In all three
379 sensitivity trees, countries of group 2 of the baseline tree (zero-covid countries) were
380 grouped together and included in a larger group together with countries of group 1 of the
381 baseline tree.

variable	base 0	base 1	base 2	base 3	Cov 1	Mob 1	Mob 2	Mob 3	No Age	No Idvi	Str. Idx
Covid-19 daily cases	Green	Green	Green	Green	Green	Green	Green	Green	Green	Green	Green
Covid-19 daily deaths	Green	Green	Green	Green	Green	Green	Green	Green	Green	Green	Green
reduction of international flights	Green	Green	Green	Green	Green	Green	Green	Green	Green	Green	Green
reduction of international and domestic flights	Green	Green	Green	Green	Green	Green	Green	Green	Green	Green	Green
workplace presence reduction	Green	Green	Green	Green	Green	Green	Green	Green	Green	Green	Green
station presence reduction	Green	Green	Green	Green	Green	Green	Green	Green	Green	Green	Green
recreation place presence reduction	Green	Green	Green	Green	Green	Green	Green	Green	Green	Green	Green
home presence rise	Green	Green	Green	Green	Green	Green	Green	Green	Green	Green	Green
IDVI	Green	Green	Green	Green	Green	Green	Green	Green	Green	Green	Green
age	Green	Green	Green	Green	Green	Green	Green	Green	Green	Green	Green
RH	Green	Green	Green	Green	Green	Green	Green	Green	Green	Green	Green
T	Green	Green	Green	Green	Green	Green	Green	Green	Green	Green	Green
latitude	Green	Green	Green	Green	Green	Green	Green	Green	Green	Green	Green
longitude	Green	Green	Green	Green	Green	Green	Green	Green	Green	Green	Green
nb days of public event restrictions	Red	Red	Red	Red	Red	Red	Red	Red	Red	Red	Red
nb days of public transport restrictions	Red	Red	Red	Red	Red	Red	Red	Red	Red	Red	Red
nb days of contact tracing implementation	Red	Red	Red	Red	Red	Red	Red	Red	Red	Red	Red
nb days of facial covering requirements	Red	Red	Red	Red	Red	Red	Red	Red	Red	Red	Red
nb days of international travel restrictions	Red	Red	Red	Red	Red	Red	Red	Red	Red	Red	Red
nb days of elderly shielding	Red	Red	Red	Red	Red	Red	Red	Red	Red	Red	Red
nb days of gathering restrictions	Red	Red	Red	Red	Red	Red	Red	Red	Red	Red	Red
nb days of school closure	Red	Red	Red	Red	Red	Red	Red	Red	Red	Red	Red
nb days of stay at home requirements	Red	Red	Red	Red	Red	Red	Red	Red	Red	Red	Red
nb days of testing implementation	Red	Red	Red	Red	Red	Red	Red	Red	Red	Red	Red
nb days of workplace closure	Red	Red	Red	Red	Red	Red	Red	Red	Red	Red	Red
stringency index	Red	Red	Red	Red	Red	Red	Red	Red	Red	Red	Red
k	0.5	1	0.5	0.5	0.5	0.5	0.5	0.5	0.5	0.5	0.5
s	130	130	26	260	130	130	130	130	130	130	130
nb observations	330	335	390	279	321	330	330	330	330	330	330
nb tested predictors	20	20	20	20	20	20	20	20	19	19	10
nb selected predictors	11	11	12	11	14	9	11	11	10	11	7
Similarity index (ARI)	-	0.82	0.61	0.53	0.66	0.94	0.95	0.92	1.00	0.69	1.00

382 **Table S3. Predictors selected for 11 alternative models.** Each model includes only variables associated with a
383 colored cell, green is for the selected variables, red for the rejected ones. Additional information about the
384 parameters k, s used for the definition of the observation set is provided. Also, the similarity index is reported: it
385 measures the similarity of the five-group classifications made by each alternative model compared with the
386 reference model (*base 0*).

387 Bibliography

- 388 1. Pawlowsky-Glahn V, Egozcue JJ. BLU Estimators and Compositional Data. *Math Geol.* 2002;34: 259–274. doi:10.1023/A:1014890722372
- 389 2. Breiman L, Friedman JH, Olshen RA, Stone CJ. *Classification And Regression Trees*. 1st ed. Chapman and Hall/CRC; 1984. doi:10.1201/9781315139470
- 390 3. Therneau TM, Atkinson B, Ripley B. *rpart : Recursive Partitioning and Regression Trees*. 2015 [cited 1 Jul 2022]. Available: <https://cran.r-project.org/web/packages/rpart/rpart.pdf>
- 391 4. Antoniadis A, Lambert-Lacroix S, Poggi J-M. Random forests for global sensitivity analysis: A selective review. *Reliab Eng Syst Saf.* 2021;206: 107312. doi:10.1016/j.ress.2020.107312
- 392 5. Karlsson EA, Mook P a. N, Vandemaele K, Fitzner J, Hammond A, Cozza V, et al. Review of global influenza circulation, late 2019 to 2020, and the impact of the COVID-19 pandemic on influenza circulation. *Wkly Epidemiol Rec.* 2021; 241–265.
- 393 6. Supplementary data. Available: https://docs.google.com/spreadsheets/d/1PirC3iJ_yrlw9CoNL0_dkmXEI7DVVoJp/edit?usp=sharing&oid=112424629266716674645&rtpof=true&sd=true
- 394 7. Tamerius JD, Shaman J, Alonso WJ, Bloom-Feshbach K, Uejio CK, Comrie A, et al. Environmental Predictors of Seasonal Influenza Epidemics across Temperate and Tropical Climates. *PLOS Pathog.* 2013;9: e1003194. doi:10.1371/journal.ppat.1003194
- 395 8. Tamerius J, Nelson MI, Zhou SZ, Viboud C, Miller MA, Alonso WJ. Global Influenza Seasonality: Reconciling Patterns across Temperate and Tropical Regions. *Environ Health Perspect.* 2011;119: 439–445. doi:10.1289/ehp.1002383
- 396 9. Shek LP-C, Lee B-W. Epidemiology and seasonality of respiratory tract virus infections in the tropics. *Paediatr Respir Rev.* 2003;4: 105–111. doi:10.1016/S1526-0542(03)00024-1

- 412 10. Soebiyanto RP, Clara W, Jara J, Castillo L, Sorto OR, Marinero S, et al. The Role of
413 Temperature and Humidity on Seasonal Influenza in Tropical Areas: Guatemala, El
414 Salvador and Panama, 2008–2013. PLOS ONE. 2014;9: e100659.
415 doi:10.1371/journal.pone.0100659
416 11. Hubert L, Arabie P. Comparing partitions. J Classif. 1985;2: 193–218.
417 doi:10.1007/BF01908075